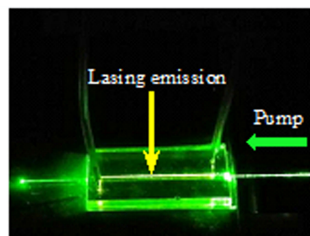


The Study on Lasing Threshold Properties of Rhodamine B in Glycerol Aqueous Solution

Volume 11, Number 2, April 2019

Yuanxian Zhang
Dongyang Li
Yonxiong Ou
Xiaoyun Pu
Yuze Sun



Evanescent wave pumped and gain coupled fiber laser

DOI: 10.1109/JPHOT.2019.2907469
1943-0655 © 2019 IEEE

The Study on Lasing Threshold Properties of Rhodamine B in Glycerol Aqueous Solution

Yuanxian Zhang ¹, Dongyang Li,¹ Yonxiong Ou,¹ Xiaoyun Pu,¹
and Yuze Sun²

¹Department of Physics, Yunnan University, Kunming 650091, China

²Department of Electrical Engineering, University of Texas at Arlington, Arlington, TX
76019 USA

DOI:10.1109/JPHOT.2019.2907469

1943-0655 © 2019 IEEE. Translations and content mining are permitted for academic research only.

Personal use is also permitted, but republication/redistribution requires IEEE permission.

See http://www.ieee.org/publications_standards/publications/rights/index.html for more information.

Manuscript received January 28, 2019; revised March 8, 2019; accepted March 21, 2019. Date of publication March 28, 2019; date of current version April 11, 2019. This work was supported in part by the National Natural Science Foundation of China under Grant 11864045, in part by the Key Research Foundation of Yunnan Province under Grant C176240210020, in part by the Young and Middle-aged Academic & Technical Leaders (Reserve Talent) in Yunnan Province under Grant 2018HB029, and in part by the China Scholarship Council Foundation. Corresponding authors: Yuanxian Zhang (e-mail: zyx74635@163.com) and Xiaoyun Pu (e-mail: xypu@163.com).

Abstract: An optical fiber is integrated in a polydimethylsiloxane substrate microfluidic channel. The laser gain medium consists of glycerol aqueous solution doped with rhodamine B (RhB) molecules, which has a lower refractive index (RI) than that of the optical fiber. The circular cross section of the optical fiber forms an optofluidic ring resonator and hosts high-quality (Q) whispering gallery modes (WGMs). Optically pumped along the fiber axis, lasing threshold properties of the RhB glycerol aqueous solution have been investigated. With the increase of both RhB dye concentration and the RI of the glycerol aqueous solution, the recorded lasing threshold decreases at first and then increases. Therefore, there is a best dye concentration as well as a best RI of the dye solution that corresponds to the lowest lasing threshold. Additionally, lasing threshold for the mixed solution of ethanol and ethylene glycol doped with RhB molecules is also demonstrated, which is much higher than that of the glycerol aqueous solution for the same dye concentration and the same RI of the dye solution. Based on evanescent wave pumped and gain coupled WGM lasing theory, we compute the lasing threshold varied with the dye concentration and the RI of the dye solution. The simulation results agree well with the experimental data.

Index Terms: Optofluidic ring resonators, lasing threshold, dye laser, glycerol aqueous solution.

1. Introduction

Over the past decades, with the increasing demand of bio-sensing, chemical analysis, and biomedical research, various optofluidic laser devices have been developed and extensively studied [1]–[7]. Particularly, optofluidic ring resonators (OFRRs) have been widely studied owing to their key merits of miniaturized size, easy to design and fabricate, and high quality (Q) factors [8]–[10]. Generally, organic dyes have been widely exploited as OFRRs laser gain medium in those aforementioned applications. The solvent of the dye directly affects the fluorescence quantum yield of the dye, the lasing threshold and the tuning range of the emitted lasing wavelength [11]–[13]. Therefore, the choice of the solvent for the dyes is significantly important. In the wavelength range of

578–610 nm, rhodamine B (RhB) has usually been selected as OFRR laser gain medium, and commonly dissolved in solvents such as pure water, ethanol, ethylene glycol and glycerol. Nevertheless, the quantum yield of RhB is only approximately 25% in pure water and 40% to 70% in ethanol or ethylene glycol at room temperature (25 °C) [14]. However, the quantum yield of RhB is close to 100% in glycerol solution [14], suggesting that it can possibly serve as the desired dye solvent. While the only drawback is that the glycerol is too viscous and easy to bubble that it is difficult to be used as a practical dye solvent. One way to solve this problem is to dilute glycerol with water to lower the viscosity. The glycerol aqueous solution formed in appropriate proportions is used as the solvent for the RhB, which not only has the advantages of excellent fluorescence quantum yield, but also avoids the viscosity and bubbles in the pure glycerol, resulting in a significantly lower lasing threshold than that of the pure ethanol or ethylene glycol as a solvent. However, to the best of our knowledge, the performance of glycerol aqueous solution as a solvent of RhB dye in an OFRR laser has rarely been explored.

The OFRR laser for the study of solvent selection of RhB used in this work is the evanescent wave pumped and gain coupled fiber laser (EPGCFL). The conventional EPGCFL is formed by inserting a fiber into a capillary tube filled with a low refractive index (RI) gain medium [15]. Although considerable progress has been made in both experimental and theoretical aspects of the EPGCFL [10], [15], [16], to date it has two major drawbacks: (i) the fiber is always suspended in the gain medium, which is difficult to keep mechanical stability of the ring resonator for manual manipulation so that it is challenging to mount the fiber on a chip; (ii) to avoid photobleaching, dye solution should be refreshed frequently which consumes large amount of dye solutions. In the present paper, we address these issues by integrating a segment optical fiber in a polydimethylsiloxane (PDMS) substrate microfluidic channel, in which the lower RI gain medium is passed through the microfluidic channel. The circular cross section of the fiber forms a ring resonator that supports high-Q whispering gallery modes (WGMs), thus providing an excellent feedback for low threshold lasing. In EPGCFL, the lasing threshold strongly relies on the dye concentration and the RI of the solution. On one hand, with the increase of the dye concentration, the lasing gain and the absorption loss of the ring resonator increase simultaneously, thus there should be a best dye concentration that results in a minimum lasing threshold. On the other hand, with the increase of RI of the solution, the lasing gain is also increased due to more evanescent wave extending into the gain medium. With the depth of potential well which confines photons in a WGM becomes lower, the photons in the WGM escape easily from the ring resonator, which directly affects the radiation loss of the laser. Accordingly, there should also be a best RI of the dye solution that results in a minimum lasing threshold. In this work, we choose the glycerol aqueous solution as the solvent of RhB and demonstrate experimentally how the EPGCFL lasing threshold properties are affected by both dye concentration and the RI of the dye solution. Meanwhile, as a contrast experimental, the lasing threshold for the mixed solution of ethanol and ethylene glycol used as solvent of RhB molecules are also demonstrated.

2. Chip Design and Fabrication

As shown in Fig. 1, The PDMS substrate was fabricated by using the population replica molding method, an inexpensive soft lithography technique. The size of the PDMS substrate was 34 mm × 15 mm (length × width), while the dimensions of the fiber channel buried in the PDMS substrate were 34 mm × 0.2 mm × 0.2 mm (length × width × height), and the microfluidic channel was 20 mm × 0.3 mm × 0.3 mm. The optical fiber was located at the center of the microfluidic channel. For the convenience of fluidic circulation in the microfluidic channel, the gap between the fiber and the fiber channel outside the microfluidic channel was blocked by the PDMS prepolymer, as shown in Fig. 1 by the dotted lines. The fabrication of the blocking process was as follows. Firstly, a segment optical fiber (length = 50 mm, diameter = 188 μm, RI $n_1 = 1.458$) was inserted in the fiber channel, and two drops of liquid PDMS prepolymer (RI = 1.41) were added into the left and the right end of the fiber channel, respectively. Then the liquid PDMS prepolymer was introduced into the fiber channel by capillarity. When the PDMS prepolymer moved to the microfluidic channel interface

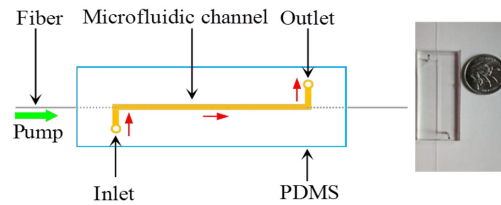


Fig. 1. Top view of an EPGCFL. The right inset shows an actual PDMS laser substrate. The dimensions of the central microfluidic channel are 20 mm \times 0.3 mm \times 0.3 mm (length \times width \times height).

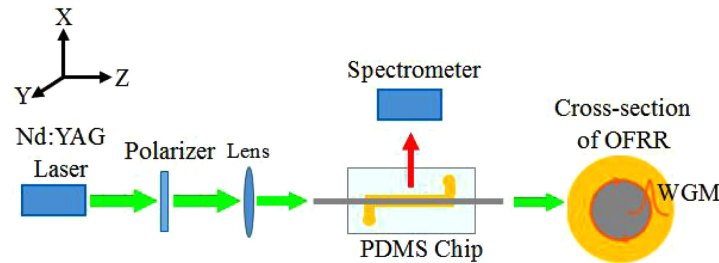


Fig. 2. A schematic diagram experimental setup of an EPGCFL. The right inset shows the cross section of the OFRR.

position as shown in Fig. 1, we covered the outlet and the inlet of the microfluidic channel by using a PDMS membrane, which can stop the moving of the PDMS prepolymer effectively. The residual PDMS prepolymer in both ends of PDMS was removed carefully by suction and scraped before curing. Secondly, the PDMS membrane was peeled from the outlet and the inlet, followed by curing at 70 °C for 45 min. Owing to the surface tension and large viscosity of the PDMS prepolymer, the liquid interface between the fiber channel and the microfluidic channel was stable during the curing process. The outlet and the inlet of the microfluidic channel in the PDMS substrate were two cylindrical holes (radius = 0.15 mm, height = 0.4 mm), which were connected to a peristaltic micro-pump (BT100-2J). The cleaning of the microfluidic channel and the liquid injection were achieved by the peristaltic micro-pump. When the microfluidic channel was subsequently filled with liquid of lower RI dye solution than that of the fiber, an EPGCFL on the PDMS chip can be formed.

3. Experiment

The experimental setup of the EPGCFL is illustrated in Fig. 2. The detail of the experimental setup is described in Ref. [15]. Here, RhB is employed as the gain medium, and the glycerol aqueous solution (RI $n_2 = 1.415$, dye concentration = 0.5 mM) is used as the solvent. The dye solution is passed through the microfluidic channel at a flow rate of 1 $\mu\text{L}/\text{min}$. A 532 nm green beam generated by a frequency doubled and Q-switched Nd:YAG laser (6 ns pulse width and 10 Hz repetition rate) is used as the pump source. The pump intensity is adjusted by a polarizer. The pump beam is longitudinally coupled into the fiber along the fiber axis by a lens (focus length 75 mm). Due to the RI of used fiber ($n_1 = 1.458$) is larger than that of the surrounding dye solution ($n_2 = 1.415$), the beam inside the fiber would propagate within fiber by total internal refraction (TIR). The evanescent field of the pump light extends out of the fiber and excites dye molecules in the dye solution, the WGMs circulate along the circumference of the OFRR cross section and provides the optical feedback for lasing. The emission light is collected along the X axis through an optical fiber and sent to a spectrometer (Spectrapro 500i) mounted with an ICCD detector (PI-Max 1024RB).

Fig. 3(a) shows an actual photograph of the EPGCFL in operation. As shown in Fig. 3(b), at low pump energy density (0.7 $\mu\text{J}/\text{mm}^2$), only a weak fluorescence emission is observed around the fiber in the microfluidic channel, and the output spectrum is broad and does not have any

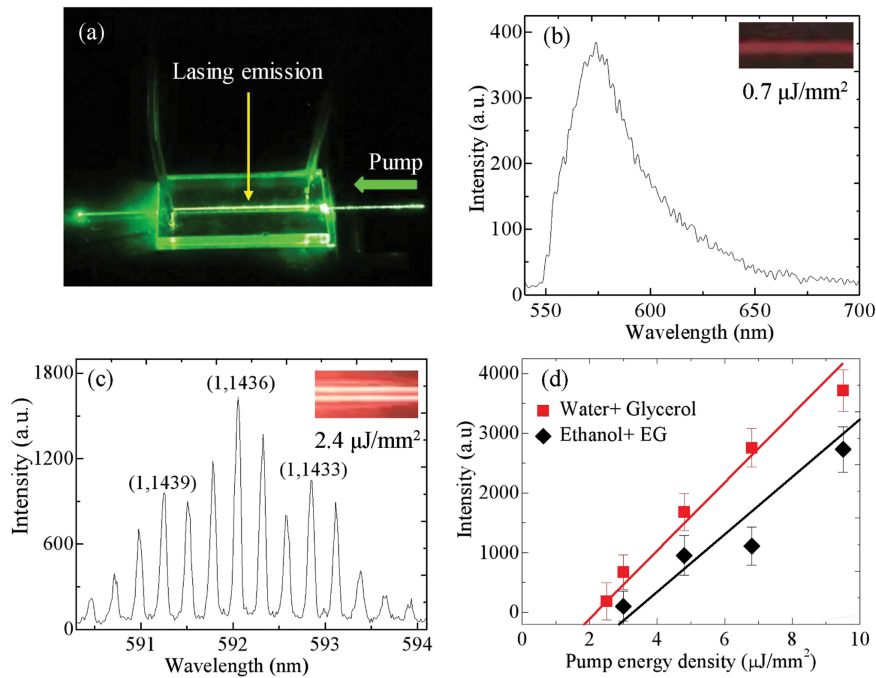


Fig. 3. (a) A photograph of the EPGCFL in operation. (b) Emission spectra below the pump threshold. Inset: weak fluorescence emission around the fiber when the pump energy density is $0.7 \mu\text{J}/\text{mm}^2$. (c) Lasing spectra over the pump threshold. Inset: strong deep-yellow lasing emission around the fiber when the pump energy density is $2.4 \mu\text{J}/\text{mm}^2$. (d) Intensity of the lasing emission vs the pump energy density. The threshold based on the linear fit (solid lines) is 1.88 and $2.85 \mu\text{J}/\text{mm}^2$, respectively. Red squares: glycerol aqueous solution is used as the solvent of RhB, black diamonds prismatic: the mixed solution of ethanol and ethylene glycol is used as the solvent of RhB. The dye concentration and the RI of the solution are 0.5mM and 1.415 , respectively. Error bars are obtained with three measurements.

mode structure. When the pump energy density surpasses a threshold value (shown in Fig. 3(c)), a strong deep-yellow light emitting from the rim of the fiber is observed in the vertical direction to the fiber axis (XY plane), and the recorded spectrum dramatically changed. A set of sharp peaks emerged with a spacing $\sim 0.39 \text{ nm}$, corresponding to the theoretical spacing $\sim \lambda^2/(2\pi n_1 a)$, where λ ($=592.5 \text{ nm}$), n_1 ($=1.458$), and a ($=94 \mu\text{m}$) are the lasing central wavelength, the RI of the fiber, and the ring resonator radius, respectively. In addition, the intensity of the lasing emission dramatically increases, with a linear dependence on the pump energy density (shown in Fig. 3(d)). All these are strong evidence of WGM lasing emission. The polarization analysis for the lasing spectra reveals that the WGM lasing emission is a typical transverse electric (TE) wave [10]. Based on the asymptotic formula (Eq. (1)) [15] for the resonant positions of WGMs in a ring resonator, the modes in the lasing spectra in Fig. 3(c) have been assigned by the radial mode order (l) and the azimuth mode number (n), where a_l is the roots of Airy function, λ_l^n is the resonant wavelength which is determined by the dye concentration and the RI of the dye solution for a fixed ring resonator diameter.

$$\frac{2\pi a n_1}{\lambda_l^n} \approx n + 2^{-1/3} a_l n^{1/3} + \frac{3}{10} 2^{-2/3} a_l^2 n^{-1/3} - \frac{n_2^2}{n_1 (n_1^2 - n_2^2)^{1/2}} + o^{-2/3}. \quad (1)$$

As a contrast, lasing threshold for the mixed solution of ethanol and ethylene glycol used as the solvent of RhB has also been investigated. As shown in black diamonds prismatic in Fig. 3(d), for the same dye concentration (0.5 mM) and the same RI (1.415) of the dye solution, the threshold based on the linear fit is approximately $2.85 \mu\text{J}/\text{mm}^2$, much higher than that of the glycerol aqueous solution used as solvent of RhB, which is approximately $1.88 \mu\text{J}/\text{mm}^2$.

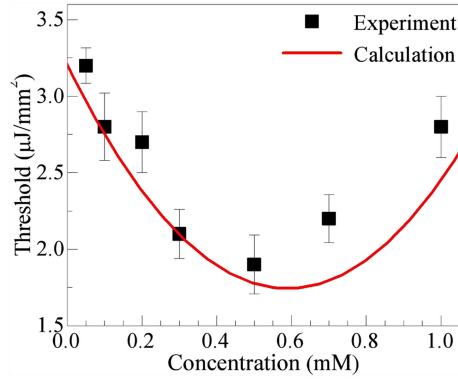


Fig. 4. Lasing threshold as a function of the dye concentration. Solid curve corresponds to the theoretical calculation result. Error bars are obtained with three measurements.

3.1 Lasing Threshold Dependence on Dye Concentration

3.1.1 Experimental Results: Fig. 4 presents the experimental results of the lasing threshold under different dye concentrations, while the RI of the dye solution is fixed at 1.415. The results reveal that the lasing threshold decrease gradually with the increase of the dye concentration when it is from 0.05 mM to 0.5 mM, beyond the value of 0.5 mM, the threshold increase significantly. There is a minimum threshold value ($1.88 \mu\text{J}/\text{mm}^2$) corresponding to the dye concentration of 0.5 mM.

3.1.2 Theoretical Analysis: Under the condition of evanescent wave pumping, when a pump beam experiences a TIR at the surface of the fiber and the dye solution, the evanescent wave of the pump light excites the dye molecules and generates an optical gain around the fiber surface within the WGM evanescent wave. The total lasing gain (G) can be expressed as [15]

$$G = \frac{CN_0\lambda_p\varepsilon_p^{th}}{4\pi \left[(n_1^2 \sin^2\theta_t - n_2^2)^{1/2} + \lambda_p\alpha_{abs}^p \right]}, \quad (2)$$

where N_0 is the dye concentration of RhB. $\lambda_p = 532 \text{ nm}$ is the wavelength of the pump light. ε_p^{th} is the pump threshold energy density. n_1 and n_2 are the RIs of the fiber and the dye solution, respectively. θ_t is the TIR angle of the pump light on the fiber interface, which is 87.4° for the used lens [15]. C is a coefficient related to the dye concentration, the fluorescence quantum efficiency of RhB dye molecules, which is a function of the central wavelength (λ_c), the RI of the dye solution, and the coupling efficiency of the pump energy density. $\alpha_{abs}^p = N_0\sigma_\alpha(\lambda)$ [15] is the absorption loss of pump light in dye solution, where $\sigma_\alpha(\lambda) \approx 2.56 \times 10^{-16} \text{ cm}^2$ is the absorption cross-section at lasing wavelength (λ_p) [15].

Fig. 5 plots of the G values varied with the dye concentration for various representative RIs of RhB dye solution based on Eq. (2), in which the ε_p^{th} value has been considered to be a constant. The simulation results indicate that when the pump light meets the TIR at the interface of the fiber, with the increase of the dye concentration, dye molecules within the evanescent field of the WGM are also increased continuously, resulting in the lasing gain increases sharply. In addition, by increasing the RI (n_2) of the cladding solution, it is beneficial to effectively increase the depth of the pump light penetrating into the dye solution, and then increase the lasing gain.

Total loss (α_{tol}) of WGM lasing in an OFRR can be written as [15]

$$\alpha_{tol} = \frac{2\pi m}{\lambda_l^n Q_{tol}}. \quad (3)$$

Where $m = n_1/n_2$. Q_{tol} is the total quality factor of the OFRR, which can be expressed approximately as $\frac{1}{Q_{tol}} \simeq \frac{1}{Q_{abs}} + \frac{1}{Q_{leak}}$. Q_{abs} and Q_{leak} are the quality factors of a ring resonator related to the energy loss coefficients α_{abs} , and α_{leak} , which are generated by cavity absorption, and light leakage,

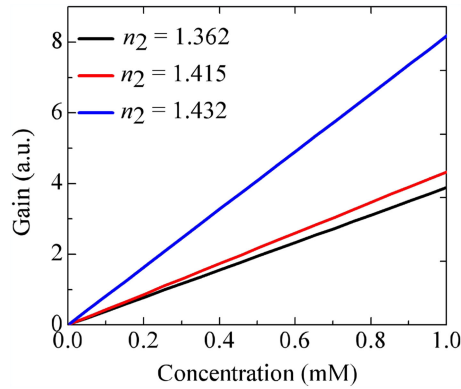
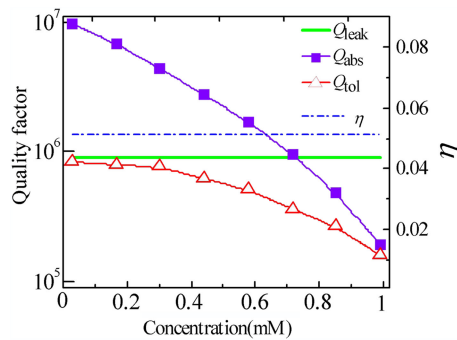


Fig. 5. Lasing gain varied with the dye concentration.

Fig. 6. Quality factors and η value varied with the dye concentration of cladding solution.

respectively. Let η be the fraction of the light in the evanescent field of the OFRR, and then the Q_{abs} can be calculated by [15]

$$Q_{abs} = \left[\frac{(1 - \eta) \lambda_l^n \alpha_{abs}^{in}}{2\pi n_1} + \frac{\eta \lambda_l^n \alpha_{abs}^{out}}{2\pi n_2} \right]^{-1}. \quad (4)$$

Where α_{abs}^{in} and α_{abs}^{out} represent the absorption loss inside and outside of the ring resonator, respectively. In the wavelength range of 578–610 nm for RhB, $\alpha_{abs}^{in} \simeq 0.0002 \text{ cm}^{-1}$ in our calculation, $\alpha_{abs}^{out} \simeq 0.132$ to 1.24 cm^{-1} for the dye concentration of 0.05 to 1 mM.

For the TE wave, the Q_{leak} can be expressed as [15]

$$Q_{leak} \simeq \frac{\pi}{4} (n_1^2 - n_2^2) x_{l,n}^2 |H_n^{(1)}(n_2 x_{l,n})|^2 \left[\left(\frac{n}{n_2 x_{l,n}} \right)^2 + \left(\frac{Y_n'(n_2 x_{l,n})}{Y_n(n_2 x_{l,n})} \right)^2 \right]. \quad (5)$$

Where $x_{l,n} = 2\pi a / \lambda_l^n$ is the size parameter of a ring resonator of radius a .

The quality factors and the η value as the function of the dye concentration are depicted in Fig. 6 (Q_{abs} in violet line + square, Q_{leak} in green solid line, Q_{tol} in red line + triangle). The calculated results reveal that the Q_{tol} is decided mainly by the Q_{leak} if the dye concentration is smaller than 0.5 mM, while it is decided mainly by the Q_{abs} if the dye concentration is larger than 0.5 mM, resulting in a sharp increase of the ring resonator loss.

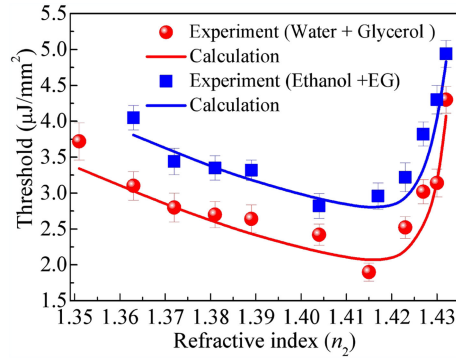


Fig. 7. Lasing threshold as a function of the RI of the dye solution. Solid curve corresponds to the theoretical calculation result. Error bars are obtained with five measurements.

At the lasing threshold, we have $G = \alpha_{tol}$. Let Eq. (2) be equal to Eq. (3), the lasing threshold energy density can be written as

$$\varepsilon_p^{th} = \frac{C' m \left[(n_1^2 \sin^2 \theta_t - n_2^2)^{\frac{1}{2}} + \lambda_p \alpha_{abs}^p \right]}{N_0 \lambda_p \lambda_l^n Q_{tol}}. \quad (6)$$

The threshold energy density as a function of dye concentration (N_0) can be calculated by Eq. (6). Each parameter is known except the coefficient $C' = 8\pi^2/C$ in Eq. (6). Here, the coupling efficiency of the pump energy density is invariable, because the fiber diameter in our experimental is a fixed value. Therefore, C' is treated approximately as $C'(N_0, \lambda_c)$. A pair of experimental data (N_0, ε_p^{th}) and the related λ_l^n and Q_{tol} value are substituted into Eq. (6) to decide C' . The parameters are chosen as follow: the central wavelength $\lambda_c = \lambda_1^{1436} = 592.054$ nm, ($N_0, \varepsilon_p^{th}, Q_{tol}$) = (0.3 mM, $2.2 \mu\text{J}/\text{mm}^2$, 8.8×10^5), then the calculated $C' \approx 1.02 \times 10^{14} \mu\text{J}/\text{mm}^3$. The experimental threshold energy density is then fitted by the red solid curve calculated from Eq. (6). It can be seen that the experimentally measured results agree well with the theory.

3.2 Lasing Threshold Dependence on RI of Dye Solution

3.2.1 Experimental Results: The experimental results of lasing threshold under various n_2 values are shown in Fig. 7 by the red dot points, and the N_0 value is fixed at 0.5 mM. The experimental results are very similar to Ref. [15] and the first experiment described in Fig. 4. That is, the lasing thresholds first decrease and then increase with the increase of the n_2 value. There is a minimum threshold energy density ($1.88 \mu\text{J}/\text{mm}^2$) when n_2 is equal to 1.415.

As a contrast experiment, lasing threshold for the mixed solution of ethanol and ethylene glycol (EG) doped with RhB molecules are also demonstrated in Fig. 7 by the blue square points. The lasing threshold of which is much higher than that of the glycerol aqueous solution for the same N_0 and the same RI of the dye solution.

3.2.2 Theoretical analysis: The quality factors and the η value as the function of the n_2 value are depicted in Fig. 8 (Q_{abs} in violet line + square, Q_{leak} in green solid line, Q_{tol} in red line + triangle). The calculated results indicate that the Q_{tol} decreases gradually with the increase of the RI of the dye solution. The Q_{tol} is decided mainly by the Q_{abs} ($\sim 10^6$) if the RI value smaller than 1.415, while it is decided mainly by the Q_{leak} if the RI larger than 1.415, resulting in an increase of the ring resonator loss.

The experimental threshold energy density (shown in Fig. 7) is fitted by the red solid curve for glycerol aqueous solvent and the blue solid curve for ethanol and ethylene glycol mixed solvent calculated from Eq. (6). The fitting methods are the same as the aforementioned method in Fig. 4. As shown in Fig. 7, the experimentally measured results are also in agreement well with the theory.

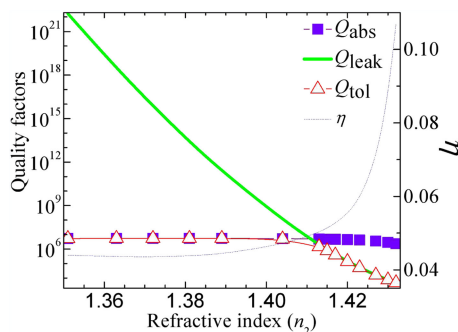


Fig. 8. Quality factors and η value varied with the RI of cladding solution.

TABLE 1
Characteristics of RhB in Several Representative Solvents

Solvents	Pure water	Glycerol	Ethanol	Ethylene glycol	References
Fluorescence quantum yield (%) 25°C	~25	~100	40~60	50~70	[14]
Viscosity coefficient (10-2pas) (20°C)	1.793	493.7	1.716	8.77	[17]

4. Discussion

As depicted in Figs. 4–6, on one hand, the cavity loss is determined mainly by the Q_{leak} if the N_0 value smaller than 0.5 mM, and the Q_{leak} is always a constant for a fixed RI of the dye solution. The lasing gain increases monotonously with the increase of N_0 . Thus, the increase of N_0 value is greatly beneficial to reduce the lasing threshold. On the other hand, the cavity loss is determined mainly by the absorption loss (Q_{abs}) if the N_0 value increases further (larger than 0.5 mM). The increased lasing gain has to compensate the increased absorption loss, meaning that more pump energy density is required to maintain the lasing threshold. Therefore, there is a best dye concentration (0.5 mM) corresponding to the minimum threshold energy density $1.88 \mu\text{J}/\text{mm}^2$.

As depicted in Figs. 5, 7 and 8, when the n_2 value is smaller than 1.415, with the increase of the n_2 value, the cavity loss is determined mainly by the slightly increased absorption loss (α_{abs}), and the lasing gain is also increased constantly with the increase of n_2 value. In this case, the increased α_{abs} and the lasing gain are greatly beneficial to reduce the lasing threshold. However, when the n_2 value is larger than 1.415, the cavity loss is determined mainly by the sharply increased leakage loss (α_{leak}), meaning that the depth of potential well which confines photons in a WGM becomes low and leading to the photons in the WGM to escape easily from ring resonator. Therefore, the pump threshold energy density is increased accordingly to compensate the increased cavity loss. Therefore, there is a best RI (1.415) of dye solution corresponds to the minimum threshold energy density ($1.88 \mu\text{J}/\text{mm}^2$).

Under a certain dye concentration and RI of dye solution, the lasing threshold is mainly decided by the fluorescence quantum yield of the dye molecules. Table 1 provides the fluorescence quantum yields of RhB in several representative solvents, in which the fluorescence quantum yield of RhB is closely related to the viscosity of the solvent, i.e., the larger the viscosity is, the higher the

fluorescence quantum yield will be. As shown in Table 1, the fluorescence quantum yield of RhB in glycerol solution is even close to 100% at room temperature (25 °C), suggesting that it is a desired solvent for improving the fluorescence quantum efficiency of the RhB. However, the glycerol is too viscous and easy to bubble and is difficult to be used as a practical dye solvent. Here, we take advantage of the merits of glycerol and pure water, which are mixed in appropriate proportions and used as the solvent of RhB. This method not only has the advantages of good fluorescence quantum yield and larger refractive index adjustment range, but also can avoid the viscosity and bubble of glycerol, resulting in a significantly lower lasing threshold than the mixed solution of ethanol and ethylene glycol as a solvent of RhB.

5. Summary

In summary, we have successfully designed and fabricated an EPGCFL chip. We have investigated the lasing threshold characteristics of RhB gain in mixed solutions. With the increase of dye concentration and the RI of the dye solution, the recorded lasing threshold first decreases and then increases, resulting in a best dye concentration as well as a best RI of the dye solution that corresponds to the minimum lasing threshold. Particularly, the glycerol aqueous solution offers advantageous features compared to the popular mixed solution of ethanol and ethylene glycol, such as a larger refractive index adjustment range, and a lower lasing threshold. Therefore, the EPGCFL chip used in this work can be an attractive candidate for various photonics applications that require sustainable, low threshold and low cost coherent light sources.

References

- [1] M. Humar and S. H. Yun, "Intracellular microlasers," *Nat. Photon.*, vol. 9, pp. 572–576, 2015.
- [2] M. G. Hansen and A. Kristensen, "Tunability of optofluidic distributed feedback dye lasers," *Opt. Exp.*, vol. 15, no. 1, pp. 137–142, 2007.
- [3] M. Humar and S. H. Yun, "Whispering-gallery-mode emission from biological luminescent protein microcavity assemblies," *Optica*, vol. 4, no. 2, pp. 222–228, 2017.
- [4] X. Fan and S. H. Yun, "The potential of optofluidic biolasers," *Nat. Methods*, vol. 11, no. 2, pp. 141–147, 2014.
- [5] L. L. Paze, K. S. Carracedo, and M. H. Rodriguez, "Liquid whispering-gallery-mode resonator as a humidity sensor," *Opt. Exp.*, vol. 25, no. 2, pp. 1165–1172, 2017.
- [6] S. Avino *et al.*, "Direct sensing in liquids using whispering-gallery-mode droplet resonator," *Adv. Opt. Mater.*, vol. 2, no. 12, pp. 1155–1159, 2014.
- [7] Ming Li, X. Wu, L. Liu, X. Fan, and L. Xu, "Self-referencing optofluidic ring resonator sensor for highly sensitive biomolecular detection," *Anal. Chem.*, vol. 85, no. 19, pp. 9328–9332, 2013.
- [8] H. Zhang, A. Balram, D. D. Meng, and Y. Sun, "Optofluidic lasers with monolayer gain at the liquid-liquid interface," *ACS Photon.*, vol. 4, no. 3, pp. 621–625, 2017.
- [9] Y. X. Zhang, X. Y. Pu, L. Feng, D. Han, and Y. Ren, "Polarization characteristics of whispering gallery mode fiber lasers based on evanescent wave coupled gain," *Opt. Exp.*, vol. 21, no. 10, pp. 12617–12628, 2013.
- [10] H. Sun *et al.*, "Fabrication of lasing whispering gallery mode microresonators by controllable injection method," *IEEE Photon. J.*, vol. 9, no. 3, Jun. 2017, Art. no. 1503006.
- [11] S. Balslev and A. Kristensen, "Microfluidic single-mode laser using high-order Bragg grating and antiguiding segments," *Opt. Exp.*, vol. 13, no. 1, pp. 344–351, 2005.
- [12] M. G. Hansen and A. Kristensen, "Tunability of optofluidic distributed feedback dye lasers," *Opt. Exp.*, vol. 15, no. 1, pp. 137–142, 2007.
- [13] J. D. Suter, Y. Sun, D. Howard, J. Viator, and X. Fan, "PDMS embedded opto-fluidic microring resonator lasers," *Opt. Exp.*, vol. 16, no. 14, pp. 10248–10253, 2008.
- [14] F. P. Schäfer, *Dye Laser*. New York, NY, USA: Springer, 1973.
- [15] Y. X. Zhang, X. Y. Pu, K. Zhu, and L. Feng, "Threshold property of whispering-gallery-mode fiber lasers pumped by evanescent waves," *J. Opt. Soc. Amer. B*, vol. 28, no. 8, pp. 2048–2056, 2011.
- [16] Y. X. Zhang, X. Y. Pu, L. Zhou, and L. Feng, "Cavity-Q-driven phenomena in an evanescent-wave pumped and gain coupled whispering-gallery-mode fiber laser," *Opt. Commun.*, vol. 285, pp. 3510–3513, 2012.
- [17] P. Pringsheim, *Flourescence and Phosphorescence*. Hoboken, NJ, USA: Wiley, 1949.